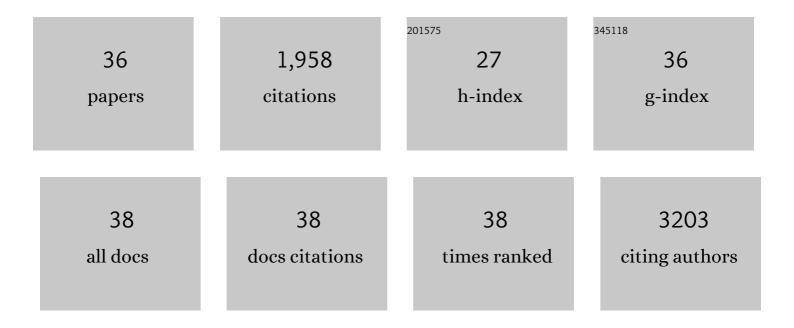
## Zhenzi Li

List of Publications by Year in descending order

Source: https://exaly.com/author-pdf/8601230/publications.pdf Version: 2024-02-01



#	Article	IF	CITATIONS
1	Dual plasmons-promoted electron-hole separation for direct Z-scheme Bi3O4Cl/AgCl heterojunction ultrathin nanosheets and enhanced photocatalytic-photothermal performance. Journal of Hazardous Materials, 2020, 384, 121268.	6.5	34
2	NormAE: Deep Adversarial Learning Model to Remove Batch Effects in Liquid Chromatography Mass Spectrometry-Based Metabolomics Data. Analytical Chemistry, 2020, 92, 5082-5090.	3.2	32
3	Identification immunophenotyping of lung adenocarcinomas based on the tumor microenvironment. Journal of Cellular Biochemistry, 2020, 121, 4569-4579.	1.2	13
4	Wide spectral response photothermal catalysis-fenton coupling systems with 3D hierarchical Fe3O4/Ag/Bi2MoO6 ternary hetero-superstructural magnetic microspheres for efficient high-toxic organic pollutants removal. Journal of Colloid and Interface Science, 2019, 533, 24-33.	5.0	61
5	Surface-defect-rich mesoporous NH2-MIL-125 (Ti)@Bi2MoO6 core-shell heterojunction with improved charge separation and enhanced visible-light-driven photocatalytic performance. Journal of Colloid and Interface Science, 2019, 554, 324-334.	5.0	44
6	Oxygen-Doped MoS <sub>2</sub> Nanospheres/CdS Quantum Dots/g-C <sub>3</sub> N <sub>4</sub> Nanosheets Super-Architectures for Prolonged Charge Lifetime and Enhanced Visible-Light-Driven Photocatalytic Performance. ACS Applied Materials & Interfaces, 2019, 11, 7104-7111.	4.0	122
7	All-Solid Z-Scheme Bi–BiOCl/AgCl Heterojunction Microspheres for Improved Electron–Hole Separation and Enhanced Visible Light-Driven Photocatalytic Performance. Langmuir, 2019, 35, 7887-7895.	1.6	39
8	Nano-zero-valent iron and MnOx selective deposition on BiVO4 decahedron superstructures for promoted spatial charge separation and exceptional catalytic activity in visible-light-driven photocatalysis-Fenton coupling system. Journal of Hazardous Materials, 2019, 377, 330-340.	6.5	48
9	WavelCA: A novel algorithm to remove batch effects for large-scale untargeted metabolomics data based on wavelet analysis. Analytica Chimica Acta, 2019, 1061, 60-69.	2.6	40
10	Surface plasma Ag-decorated single-crystalline TiO2â^'x(B) nanorod/defect-rich g-C3N4 nanosheet ternary superstructure 3D heterojunctions as enhanced visible-light-driven photocatalyst. Journal of Colloid and Interface Science, 2019, 542, 63-72.	5.0	31
11	Plasmon Ag and CdS quantum dot co-decorated 3D hierarchical ball-flower-like Bi <sub>5</sub> O <sub>7</sub> I nanosheets as tandem heterojunctions for enhanced photothermal–photocatalytic performance. Catalysis Science and Technology, 2019, 9, 6714-6722.	2.1	29
12	Bifunctional nest-like self-floating microreactor for enhanced photothermal catalysis and biocatalysis. Environmental Science: Nano, 2019, 6, 3551-3559.	2.2	13
13	Assembly of surface-defect single-crystalline strontium titanate nanocubes acting as molecular bricks onto surface-defect single-crystalline titanium dioxide (B) nanorods for efficient visible-light-driven photocatalytic performance. Journal of Colloid and Interface Science, 2019, 537, 441-449.	5.0	10
14	Synergistic effect of surface plasmon resonance, Ti3+ and oxygen vacancy defects on Ag/MoS2/TiO2-x ternary heterojunctions with enhancing photothermal catalysis for low-temperature wastewater degradation. Journal of Hazardous Materials, 2019, 364, 117-124.	6.5	93
15	C,N co-doped porous TiO <sub>2</sub> hollow sphere visible light photocatalysts for efficient removal of highly toxic phenolic pollutants. Dalton Transactions, 2018, 47, 4877-4884.	1.6	26
16	Plasmon Ag decorated 3D urchinlike N-TiO2â^'x for enhanced visible-light-driven photocatalytic performance. Journal of Colloid and Interface Science, 2018, 521, 102-110.	5.0	25
17	Mesoporous black TiO2-x/Ag nanospheres coupled with g-C3N4 nanosheets as 3D/2D ternary heterojunctions visible light photocatalysts. Journal of Hazardous Materials, 2018, 343, 181-190.	6.5	147
18	Sites of distant metastases and overall survival in ovarian cancer: A study of 1481 patients. Gynecologic Oncology, 2018, 150, 460-465.	0.6	100

Zhenzi Li

#	Article	IF	CITATIONS
19	Identification of pathwayâ€based recurrenceâ€associated signatures in optimally debulked patients with serous ovarian cancer. Journal of Cellular Biochemistry, 2018, 119, 8564-8573.	1.2	Ο
20	3D urchin-like black TiO <sub>2â^'x</sub> /carbon nanotube heterostructures as efficient visible-light-driven photocatalysts. RSC Advances, 2017, 7, 453-460.	1.7	35
21	Black TiO2 nanobelts/g-C3N4 nanosheets Laminated Heterojunctions with Efficient Visible-Light-Driven Photocatalytic Performance. Scientific Reports, 2017, 7, 41978.	1.6	211
22	Identification of a six-IncRNA signature associated with recurrence of ovarian cancer. Scientific Reports, 2017, 7, 752.	1.6	52
23	808 nm light triggered black TiO2 nanoparticles for killing of bladder cancer cells. Materials Science and Engineering C, 2017, 81, 252-260.	3.8	46
24	Ti3+ self-doped mesoporous black TiO2/graphene assemblies for unpredicted-high solar-driven photocatalytic hydrogen evolution. Journal of Colloid and Interface Science, 2017, 505, 1031-1038.	5.0	42
25	In Situ Ti <sup>3+</sup> /N-Codoped Three-Dimensional (3D) Urchinlike Black TiO <sub>2</sub> Architectures as Efficient Visible-Light-Driven Photocatalysts. Industrial & Engineering Chemistry Research, 2017, 56, 7948-7956.	1.8	32
26	Facile synthesis of high-thermostably ordered mesoporous TiO 2 /SiO 2 nanocomposites: An effective bifunctional candidate for removing arsenic contaminations. Journal of Colloid and Interface Science, 2017, 485, 32-38.	5.0	34
27	Metabolic profiling and novel plasma biomarkers for predicting survival in epithelial ovarian cancer. Oncotarget, 2017, 8, 32134-32146.	0.8	30
28	Distinct plasma lipids profiles of recurrent ovarian cancer by liquid chromatography-mass spectrometry. Oncotarget, 2017, 8, 46834-46845.	0.8	35
29	Fabrication of 3 D Mesoporous Black TiO <sub>2</sub> /MoS <sub>2</sub> /TiO <sub>2</sub> Nanosheets for Visibleâ€Lightâ€Driven Photocatalysis. ChemSusChem, 2016, 9, 1118-1124.	3.6	164
30	Superâ€hydrophilic porous TiO <sub>2</sub> â€ZnO composite thin films without light irradiation. Environmental Progress and Sustainable Energy, 2016, 35, 1121-1124.	1.3	2
31	Ti <sup>3+</sup> Self-Doped Blue TiO <sub>2</sub> (B) Single-Crystalline Nanorods for Efficient Solar-Driven Photocatalytic Performance. ACS Applied Materials & Interfaces, 2016, 8, 26851-26859.	4.0	151
32	Multifunctional Floating Titania oated Macro/Mesoporous Photocatalyst for Efficient Contaminant Removal. ChemPlusChem, 2015, 80, 623-629.	1.3	29
33	Ni <sup>2+</sup> and Ti <sup>3+</sup> co-doped porous black anatase TiO <sub>2</sub> with unprecedented-high visible-light-driven photocatalytic degradation performance. RSC Advances, 2015, 5, 107150-107157.	1.7	59
34	One-step synthesis of mesoporous two-line ferrihydrite for effective elimination of arsenic contaminants from natural water. Dalton Transactions, 2011, 40, 2062.	1.6	38
35	Facile synthesis of Ag nanoparticles supported on MWCNTs with favorable stability and their bactericidal properties. Journal of Hazardous Materials, 2011, 187, 466-472.	6.5	38
36	The high dispersion of DNA–multiwalled carbon nanotubes and their properties. Analytical Biochemistry, 2009, 387, 267-270.	1.1	51